

Observational Constraints on Silent Quartessence

Luca Amendola*

INAF/Osservatorio Astronomico di Roma, Via Frascati 33, I-00040 Monte Porzio Catone, RM, - Italy

Ioav Waga†

Universidade Federal do Rio de Janeiro, Instituto de Física, CEP 21941-972, Rio de Janeiro, RJ, Brazil

Fabio Finelli‡

INAF/IASF, Sezione di Bologna, Istituto di Astrofisica Spaziale e Fisica Cosmica,
Istituto Nazionale di Astrofisica, via Gobetti, 101 - I-40129 Bologna - Italy

(Dated: 7th November 2018)

We derive new constraints set by SNIa experiments ('gold' data sample of Riess *et al.*), X-ray galaxy cluster data (Allen *et al.* *Chandra* measurements of the X-ray gas mass fraction in 26 clusters), large scale structure (Sloan Digital Sky Survey spectrum) and cosmic microwave background (WMAP) on the quartessence Chaplygin model. We consider both adiabatic perturbations and intrinsic non-adiabatic perturbations such that the effective sound speed vanishes (*Silent Chaplygin*). We show that for the adiabatic case, only models with equation of state parameter $|\alpha| \lesssim 10^{-2}$ are allowed: this means that the allowed models are very close to Λ CDM. In the *Silent* case, however, the results are consistent with observations in a much broader range, $-0.3 < \alpha < 0.7$.

I. INTRODUCTION

Two of the major puzzles of contemporary cosmology are the nature of dark matter and of dark energy, the two big players in the cosmic arena. So far, the only knowledge of these components refers to their density fraction and to their equation of state, and even on these numbers we still have a large uncertainty. Greater still is the ignorance of their clustering properties: although we assume that essentially all the dark matter clusters in observable objects and all the dark energy does remain quite homogeneous, this is to a large extent only a simplification rather a consequence of observations.

It is therefore no surprise that many works are currently devoted to the possibility of merging the two puzzles into a single one: that is, finding a single origin for both dark matter and dark energy. A possibility is to assume an interaction between dark matter and dark energy [1] or to fit both into a single complex field [2]. However, these models still contain two separate fields that account ultimately for the two components. On a different level lies the hypothesis that there is a single fluid that behaves as dark matter or dark energy according to the background or the local density. Since there is only one unifying dark-matter-energy component, besides baryons, photons and neutrinos, this model is usually referred to as quartessence [3]. A phenomenological prototype of quartessence models is the generalized Chaplygin model [4, 5, 6], an exotic fluid with an inverse power law homogeneous equation of state (EOS), $\bar{p} = -M^{4(\alpha+1)}/\bar{\rho}^\alpha$, where M has dimension of mass and

$\alpha > -1$ is a dimensionless parameter ($\alpha = 1$ is the original Chaplygin gas). Such equation of state leads to a component which behaves as dust in the past and as cosmological constant in the future. For $\alpha = 0$ the model reduces to Λ CDM [7].

For a wide range of values of the parameter α , the quartessence Chaplygin model is compatible with several cosmological tests that involve only the background metric [8]. Nevertheless, problems may occur when one considers perturbations. For instance, the CMB anisotropies spectrum is strongly suppressed with respect to Λ CDM [9]. Further, it was shown that, unless α is very much close to $\alpha = 0$, the mass power spectrum presents strong instabilities and oscillations [10]. A quantitative CMB analysis [11] (see also [12] for a pre-WMAP analysis of the generalized Chaplygin gas as dark energy) found that the parameter α should be small ($\alpha < 0.2$ at 95% CL), even including an additional CDM component, and smaller still without the latter. We will show below that in fact this limit reduces to $|\alpha| < 0.01$. It is clear that this strong limit is due to the finite sound speed of the Chaplygin fluid: when it is sufficiently large and positive, it prevents clustering on small scales and therefore introduces a cut in the power spectrum which is at odds with observations; when it is negative, on the other hand, the clustering at small scales is enhanced beyond control.

It is important to stress, however, that unlike the background tests, the perturbation analysis need further assumptions beyond the equation of state. In [13], it was shown that it is possible to avoid the mass power spectrum problem if, for instance, pressure perturbation vanishes. This can be done by introducing a special type of intrinsic entropy perturbation such that the effective sound speed [14] of the cosmic fluid vanishes (we denote this as *silent perturbations*). We call the Chaplygin quartessence model with vanishing pressure perturbation *Silent Chaplygin* and refer to the standard case as *adia-*

*Electronic address: amendola@mporzio.astro.it

†Electronic address: ioav@if.uff.br

‡Electronic address: finelli@bo.iasf.cnr.it

batic Chaplygin.

The main goal of this paper is to show that, unlike adiabatic Chaplygin, Silent Chaplygin is consistent with CMB data for a wide range of parameters. Besides CMB, we also consider consistency of Silent Chaplygin with current data from large scale structure, from type Ia supernovae (SNIa) and baryon fraction in galaxy clusters. Using the latest data sets, we review all these tests using a careful treatment, presenting the outcome of a combined analysis of the data for both Silent and adiabatic Chaplygin.

II. BASIC EQUATIONS

In this section we give a brief and basic description of the model. The conservation equation for the generalized Chaplygin gas component in a Robertson-Walker metric is solved by

$$\bar{\rho}_{Ch} = \bar{\rho}_{Ch0}[-w_0 + \frac{1+w_0}{a^{3(\alpha+1)}}]^{\frac{1}{1+\alpha}}, \quad (1)$$

where a is the scale factor ($a = 1$ today) and $w_0 = -\frac{M^4}{\bar{\rho}_{Ch0}^{2\alpha+1}}$ is the present equation of state.

The equation-of-state parameter ($w = \bar{p}/\bar{\rho}$) and the adiabatic sound velocity ($c_s^2 = d\bar{p}/d\bar{\rho}$) for the Chaplygin gas, are given by

$$w_{Ch}(a) = \frac{w_0}{-w_0 + (1+w_0)a^{-3(\alpha+1)}} \quad (2)$$

and

$$c_{sCh}^2(a) = -\alpha w_{Ch}(a). \quad (3)$$

From the equation above, it is clear that at early times, when $a \rightarrow 0$, we have $w_{Ch} \rightarrow 0$, and the fluid behaves as non relativistic matter. At late times, when $a \gg 1$, we obtain $w_{Ch} \rightarrow -1$. Further, the adiabatic sound speed has maximum value when the equation of state parameter is minimum. Therefore, the epoch of cosmic acceleration, in these models, coincides with that of large c_s^2 . As remarked in [15], this is a characteristic of all unified models in which the equation of state is convex, i.e., is such that $\frac{d^2\bar{p}}{d\bar{\rho}^2} = \frac{dc_s^2}{d\bar{\rho}} < 0$. However, this property is not mandatory for a general fluid. Models with concavity changing equations of state, may have c_s^2 negligibly small when the energy density reaches its minimum value. This is an important property that must be considered in constructing acceptable adiabatic quartessence models [16].

The perturbation equations for a fluid with equation of state w and adiabatic sound speed c_s^2 in *synchronous* gauge are (for the sake of simplicity, here we neglect baryons and radiation, and we assume that both spatial curvature and the anisotropic perturbation vanish)

$$\delta' = -3(w\Gamma + c_s^2\delta - w\delta) - (1+w)(\theta + \frac{h'_L}{2}) \quad (4)$$

$$\theta' = \frac{k^2}{(1+w)\mathcal{H}^2}(w\Gamma + c_s^2\delta) + (3c_s^2 - 1 - \frac{\mathcal{H}'}{\mathcal{H}})\theta \quad (5)$$

$$h'_L = \frac{2k^2\eta}{\mathcal{H}^2} + 3\delta\Omega \quad (6)$$

$$\eta' = \frac{3(1+w)\mathcal{H}^2\theta\Omega}{2k^2} \quad (7)$$

where derivatives are with respect to a . Here δ is the density contrast, Ω is the density parameter, h_L and η are metric perturbations, θ is the divergence of the velocity perturbation, Γ is the entropy perturbation and $\mathcal{H} \equiv da/d\tau$, τ being the conformal time. To these equations, we must add the equations for baryons and relativistic fluid. The assumption of a *silent universe* requires that [13]

$$\delta p = \bar{p}\Gamma + c_s^2(\delta\rho) = 0$$

so that

$$\Gamma = -\frac{c_s^2}{w}\delta$$

We adopt therefore these equations with $w = w_{Ch}$ and $c_s = c_{sCh}$. With this choice, $\Gamma = \alpha\delta$ and models with $\alpha = 0$ are both, silent and adiabatic.

III. OBSERVATIONAL CONSTRAINTS

In the subsections below, we will derive constraints on the parameters α and w_0 from four data sets: SNIa, X-ray cluster gas fraction, SDSS power spectrum and CMB.

A. SNIa

The luminosity distance of a light source is defined in such a way as to generalize to an expanding and curved space the inverse-square law of brightness valid in a static Euclidean space,

$$d_L = \left(\frac{L}{4\pi\mathcal{F}}\right)^{1/2}. \quad (8)$$

In Eq. (8), L is the absolute luminosity and \mathcal{F} is the measured flux.

For a source of absolute magnitude M , the apparent bolometric magnitude $m(z)$ can be expressed as

$$\begin{aligned} m(z) &= M - 5 \log H_0 + 25 + 5 \log D_L \\ &= M + 42.3841 - 5 \log h + 5 \log D_L, \end{aligned} \quad (9)$$

where D_L is the luminosity distance in units of H_0^{-1} (we are using $c = 1$),

$$D_L = \int_0^z [E(z')]^{-1} dz', \quad (10)$$

where

$$E^2(z) = \left\{ \omega_b h^{-2} (1+z)^3 + (1 - \omega_b h^{-2}) \left[-w_0 + (1+w_0)(1+z)^{3(1+\alpha)} \right]^{\frac{1}{1+\alpha}} \right\}. \quad (11)$$

Here, z is the redshift, $\omega_b = \Omega_b h^2$, and h is the Hubble constant in units of $100 \text{ km/s Mpc}^{-1}$.

For the SNIa analysis, we use the ‘gold’ data set of Riess *et al.* [17]. The data in this sample is given in terms of the extinction corrected distance modulus, $\mu_0 = m - M$. To obtain the likelihood of the parameters, we use a χ^2 statistics such that,

$$\chi^2(\alpha, w_0, h, \omega_b) = \sum_{i=1}^{157} \left(\frac{\mu_{0,i} - 42.3841 + 5 \log h - 5 \log D_L(z_i, \alpha, w_0, h, \omega_b)}{\sigma_{\mu_{0,i}}} \right)^2. \quad (12)$$

In (12), $\sigma_{\mu_{0,i}}$ are the estimated errors in the individual distance moduli, including uncertainties in galaxy redshift and also taking into account the dispersion in supernovae redshift due to peculiar velocities (see [17] for details). To determine the likelihood of the parameters α and w_0 , we marginalize the likelihood function over h and ω_b . We use two different priors in this work. We consider flat priors when combining the SNIa and clusters results with CMB, while in this and in the next subsection we adopt Gaussian priors such that $h = 0.72 \pm 0.08$ [18] and $\omega_b = 0.0214 \pm 0.002$ [19]. The results of our SNIa analysis are displayed in Fig. 1. In the figure, we show 68% and 95% confidence level contours in the (α, w_0) plane.

B. X-ray Cluster Gas Fraction

Clusters of galaxies are the most recent large-scale structures formed and the largest gravitationally bound systems known. Therefore, the determination of their matter contents is important since cluster properties should approach those of the Universe as a whole. By measuring the baryon mass fraction Ω_b/Ω_m in rich clusters, and combining this ratio with Ω_b determinations from primordial nucleosynthesis, constraints on Ω_m can be placed [20]. Further, by assuming that baryon mass fraction in clusters of galaxies is independent of redshift, it is also possible to constrain the geometry and, consequently, the dark energy density. A method based on this idea was suggested by Sasaki [21] and Pen [22] and further developed and applied by Allen, Schmidt, and Fabian [23].

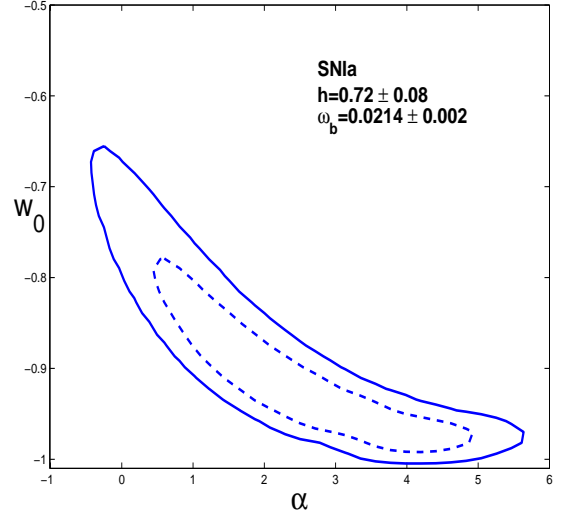


Figure 1: Constant confidence contours (68% and 95%) in the (α, w_0) plane allowed by SNIa data, as described in the text

In this section we use the new data set of Allen *et al.* [24] to constraint the Chaplygin models. These authors extracted from Chandra observations the x-ray gas mass fraction (f_{gas}) of twenty six massive, dynamically relaxed galaxy clusters, with redshifts in the range $0.08 < z < 0.9$, and that have converging f_{gas} within a radius r_{2500} (radius encompassing a region with mean mass density 2500 times the critical density of the Universe at the cluster redshift).

To determine the confidence region of the parameters of the model, we use the following χ^2 function in our computation:

$$\chi^2(\alpha, w_0, h, \omega_b, b) = \sum_{i=1}^{26} \frac{[f_{\text{gas}}^{\text{mod}}(z_i, \alpha, w_0, h, \omega_b, b) - f_{\text{gas},i}]^2}{\sigma_{f_{\text{gas},i}}^2}, \quad (13)$$

where z_i , $f_{\text{gas},i}$, and $\sigma_{f_{\text{gas},i}}$ are, respectively, the redshifts, the SCDM ($h = 0.5$) best-fitting values, and the symmetric root-mean-square errors for the 26 clusters as given in [24]. In Eq. (13), $f_{\text{gas}}^{\text{mod}}$ is the model function [23]

$$f_{\text{gas}}^{\text{mod}} = \frac{b \omega_b h^{-2}}{(1 + 0.19 \sqrt{h}) \Omega_m^{\text{eff}}} \left(\frac{h}{0.5} \frac{d_A^{\text{EdS}}}{d_A^{\alpha, A}} \right)^{3/2}. \quad (14)$$

Here, $d_A = (1+z)^{-2} d_L$ is the angular diameter distance to the cluster, b is a bias factor that takes into account the fact that the baryon fraction in clusters could be lower than for the Universe as a whole and

$$\Omega_m^{\text{eff}} = (1 - \omega_b h^{-2}) (1 + w_0)^{1/(1+\alpha)} + \omega_b h^{-2}. \quad (15)$$

is the effective matter density parameter [8]. In our computations, we first marginalize analytically over the bias factor assuming that it is Gaussian-distributed with $b = 0.824 \pm 0.089$ [24, 25]. To determine the likelihood of

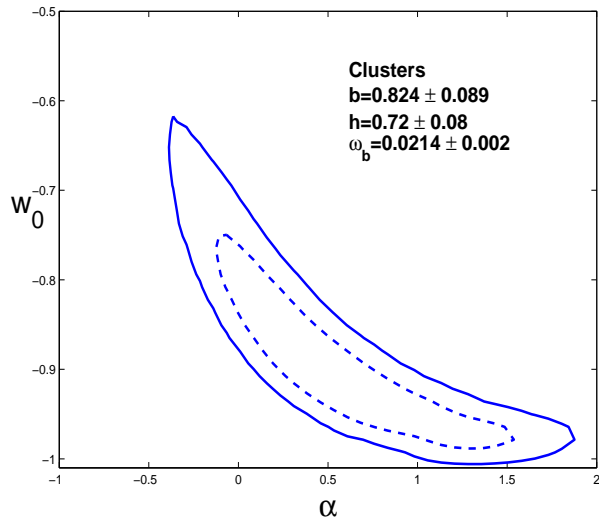


Figure 2: Constant confidence contours (68% and 95%) in the (α, w_0) plane from cluster f_{gas} data as described in the text.

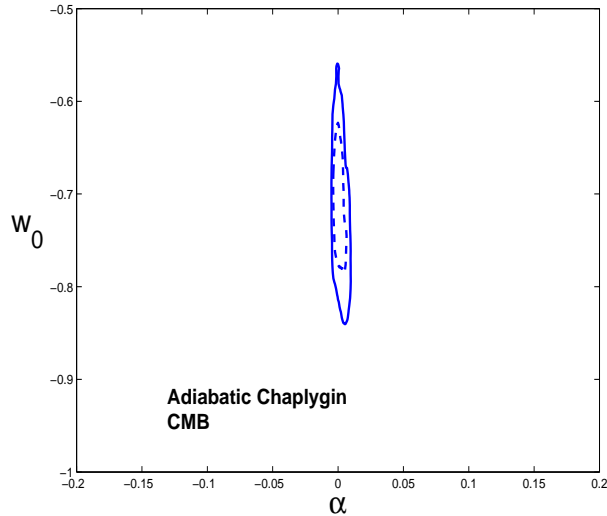


Figure 3: Constant confidence contours (68% and 95%) in the (α, w_0) plane allowed by CMB, as described in the text.

the parameters α and w_0 , we next marginalize the likelihood function over h and ω_b . As remarked before, we assume here a Gaussian prior such that $h = 0.72 \pm 0.08$ [18] and $\omega_b = 0.0214 \pm 0.002$ [19].

In Fig. 2, we show the 68% and 95% confidence contours on the parameters α and w_0 determined from the Chandra data.

C. CMB

Here we compare the model to the combined temperature and polarization power spectrum estimated by WMAP [26]. To derive the likelihood we adopt a ver-

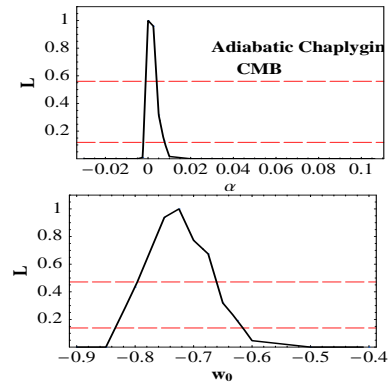


Figure 4: CMB likelihood functions for α and w_0 in the adiabatic case. The horizontal lines mark the 68% and 95% c.l., top to bottom.

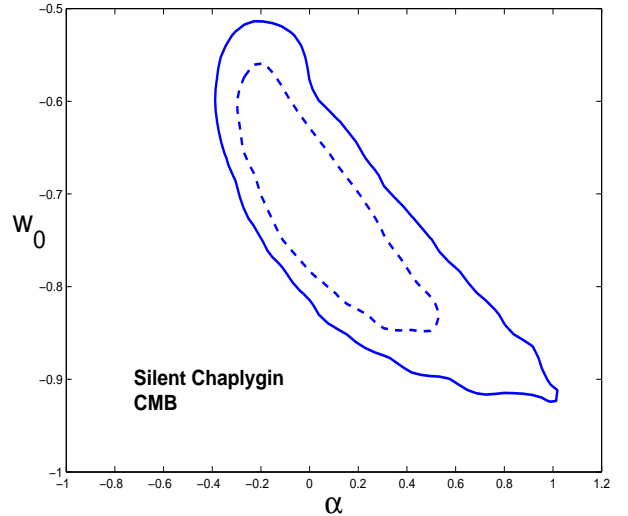


Figure 5: Constant confidence contours (68% and 95%) in the (α, w_0) plane allowed by CMB, as described in the text

sion of the routine described in Verde *et al.* [27], which takes into account all the relevant experimental properties (calibration, beam uncertainties, window functions, etc).

Our theoretical model depends on two Chaplygin parameters, four cosmological parameters and the overall normalization N :

$$\alpha, w_0, n_s, h, \omega_b, \tau, N. \quad (16)$$

The overall normalization has been integrated out numerically. We calculate the theoretical $C_{\ell,t}$ spectra by a modified parallelized CMBFAST [30] code that includes the full set of perturbation equations [9, 11] with the addition of non-adiabatic pressure perturbations. We do not include gravitational waves and the other parameters are set as follows: $T_{cmb} = 2.726K$, $Y_{He} = 0.24$, $N_\nu = 3.04$.

We evaluated the likelihood on a unequally spaced grid of roughly 50,000 models (for each normalization) with

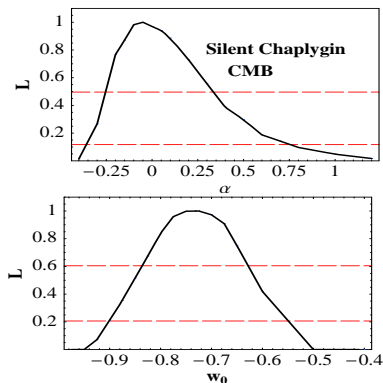


Figure 6: CMB likelihood functions for α and w_0 in the silent case. The horizontal lines mark the 68% and 95% c.l., top to bottom.

the following top-hat broad priors: $w_0 \in (-1, -0.5)$, $\alpha \in (-0.8, 1.5)$, $n_s \in (0.8, 1.2)$, $\omega_b \in (0.02, 0.025)$, $\tau \in (0, 0.3)$. For the Hubble constant we adopted the top-hat prior $h \in (0.6, 0.8)$; we also employed the HST result [18] $h = 0.72 \pm 0.08$ (Gaussian prior).

In Fig. 3, we show the confidence region on α, w_0 in the adiabatic case, after marginalization over all the other parameters with flat priors: as it can be seen, this is the most stringent test among those studied in this paper. As anticipated, it restricts α to be very close to 0: in other words, observations of CMB demands that the background of adiabatic Chaplygin be almost indistinguishable from Λ CDM. In Fig. 5 we contrast this result with the silent case: now the allowed region for α widens a lot, encompassing values close to unity. What is particularly interesting is that even with $\alpha = 1$, Silent Chaplygin is consistent at the 2σ level, while it was obviously ruled out in the adiabatic case. In Figs. 4 and 6. we show the one-dimensional likelihood for α and w_0 , with marginalization over all the other parameters.

D. Large scale structure

The results of Sandvik et al. (2004) [10] have shown that the matter power spectrum of adiabatic Chaplygin is plagued by strong instabilities and oscillations for any α significantly different from zero, leading to a stringent upper limit to $|\alpha|$. In [13], it has been shown that these problems do not occur for the silent model. To test this in a more quantitative way we perform here a simplified likelihood analysis with the following procedure. We compared the baryon spectra of the silent case to the matter power spectrum of Sloan Digital Sky Survey (SDSS) as obtained in Tegmark et al. (2004) [28], cutting at $k = 0.02h/\text{Mpc}$, using the likelihood routine provided by M. Tegmark [29], and marginalizing over the amplitude (i.e., we are comparing only the slope of the spectrum, not its absolute value). In order to save computer time we restricted ourselves to a subset of parameters, fixing

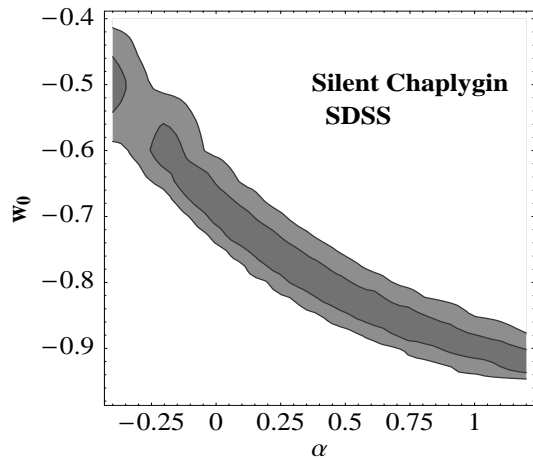


Figure 7: SDSS likelihood functions at 68% and 95 % c.l. for α and w_0 in the silent case.

$\omega_b = 0.023$, $n_s = 1$ and $h = 0.7$. As we show in Fig. 7, the results are rather similar to the CMB case. Since we used only a very small subset of the whole parameters space we will not include the SDSS likelihood in the combined likelihood of the next section. The loss in constraining power is acceptable since one can easily see that the CMB and the SDSS confidence regions are overlapping to a good extent. Moreover, extending the range of parameters as in the CMB case the SDSS constraints would become weaker and would not add much to the information from the CMB.

We also calculated the baryon fluctuation variance σ_8 (i.e. the absolute normalization of the spectrum) for the same subset of parameters. In Fig. 8 we show the contour plots of the likelihood assuming a Gaussian distribution of the observed σ_8 with $\sigma_8 = 0.9 \pm 0.1$. This test is meant to be only qualitative since the value of σ_8 that is derived from data is strongly degenerate with Ω_m and with the bias factor and/or it depends on calibration obtained with N -body simulations based on some specific cosmological model. We only notice that for the Silent Chaplygin case there exists a large region in our parameter space which accounts for values of σ_8 which are consistent with the standard estimation. It is nevertheless interesting to note that the σ_8 analysis shows preference for lower values of w_0 (for a fixed α) than the CMB test. This could help to further reduce the parameters space.

IV. COMBINED CONSTRAINTS AND CONCLUSION

Here we present a combined analysis of the constraints discussed in the previous section. In Fig. 9 we display the allowed region of the parameters w_0 and α from a combination of data from SNIa, clusters and CMB in adiabatic Chaplygin. The constraints on the parameter α are roughly the same as those obtained from CMB

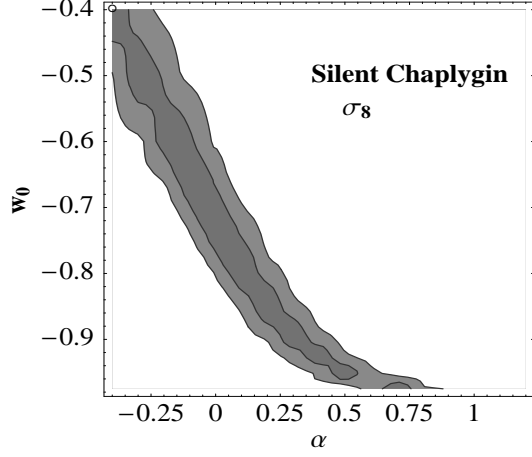


Figure 8: Likelihood function for σ_8 at 68% and 95 % c.l. for α and w_0 in the silent case.

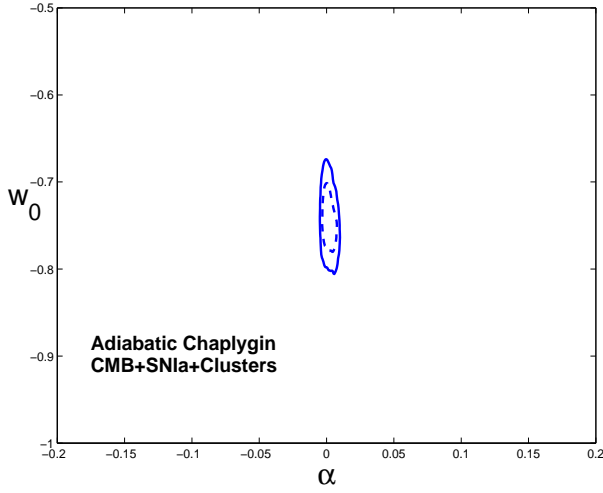


Figure 9: Constant confidence contours (68% and 95%) in the (α, w_0) plane allowed by SNIa, clusters and CMB, as described in the text.

alone. Only models with α very close to the Λ CDM limit are allowed. Although including SNIa and clusters in the CMB analysis almost do not affect the constraints on α , they tighten the constraints on the parameter w_0 , reducing even more the allowed region of the parameters space in the adiabatic case. The final result (95% c.l.) for the adiabatic case is

$$-0.005 < \alpha < .01, \quad -0.8 < w_0 < -0.7. \quad (17)$$

In contrast, in Fig. 10, the Silent Chaplygin model is consistent with the observables considered here for a wide range of parameters. The constraints in the silent case are (95% c.l.)

$$-0.25 < \alpha < 0.5, \quad -0.87 < w_0 < -0.68, \quad (18)$$

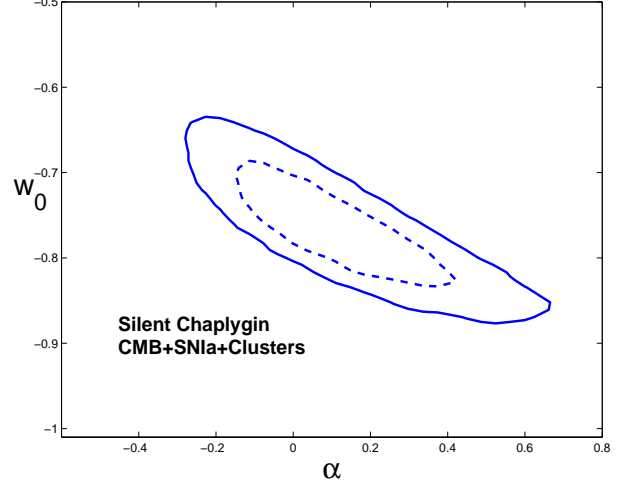


Figure 10: Constant confidence contours (68% and 95%) in the (α, w_0) plane allowed by SNIa, clusters and CMB, as described in the text

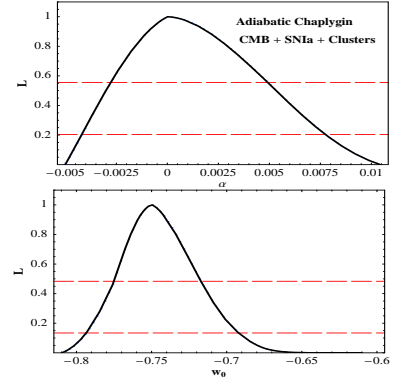


Figure 11: Likelihood functions for α and w_0 in the adiabatic case for SNIa, clusters and CMB. The horizontal lines mark the 68% and 95% c.l., top to bottom.

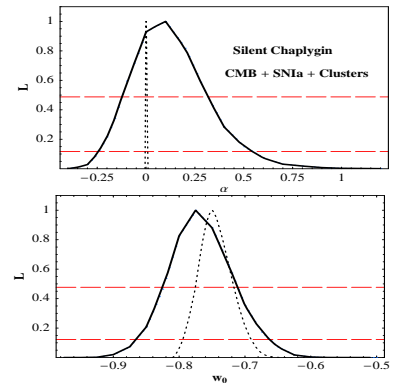


Figure 12: Likelihood functions for α and w_0 in the silent case for SNIa, clusters and CMB. The horizontal lines mark the 68% and 95% c.l., top to bottom. For comparison, we plot as dotted lines the combined likelihood functions of the adiabatic case.

with a remarkable fifty-fold extension in the range of α . The one-dimensional likelihood functions are shown in Figs. 11 and 12.

The idea of unifying dark matter and dark energy through a single component has motivated many works in the last few years. Most of these investigations concentrated their efforts in analyzing the generalized Chaplygin fluid, that is considered the prototype of the quartessence models. After the results of [9, 10, 11], it became clear that adiabatic Chaplygin, as quartessence, is ruled out unless the parameter α is very close to zero. In the present paper we confirmed this result by using current CMB data, extending the quantitative results of [11] to quartessence models. In fact, for an effective sound speed different from zero, any quartessence model with a convex EOS will suffer the same kind of problem [15]. There are two simple ways to get around this problem: choosing an EOS not convex [16] or introducing entropic perturbations as we did in this paper. This shows that indeed quartessence models of the Chaplygin type (one fluid, two parameters) can be considered as real alterna-

tives to Λ CDM (two fluids, one parameter). It is clear however that these phenomenological models should be further investigated: the challenge is to connect them to a more fundamental theory.

Finally, we remark that one possible source of problems for Silent Chaplygin is lensing skewness [31]. It would be remarkable if higher-order or non-linear effects would prove necessary to rule out, or strongly constrain, these models.

Acknowledgments

We thank Maurício Calvão, Roberto Colistete, Martin Makler and Ribamar Reis for useful discussions. The CMB computations have been performed at CINECA (Italy) under the agreement INAF@CINECA. We thank the staff for support. IW is partially supported by the Brazilian research agency CNPq.

-
- [1] L. Amendola, Phys. Rev. D **62**, 043511, (2000).
 - [2] R. Mainini & S.A. Bonometto, Phys. Rev. Lett. **93**, 121301 (2004).
 - [3] M. Makler, S.Q. Oliveira & I. Waga, Phys. Lett. B **555**, 1 (2003).
 - [4] A. Kamenshchik, U. Moschella & V. Pasquier, V., 2001, Phys. Lett. B **511**, 265 (2001).
 - [5] N. Bilić, G.B. Tupper & R.D. Viollier, Phys. Lett. B **535**, 17 (2002).
 - [6] M.C. Bento, O. Bertolami & A.A. Sen, Phys. Rev. D **66**, 043507 (2002).
 - [7] P.P. Avelino, L.M.G. Beça, J.P.M. de Carvalho & C.J.A.P. Martins, JCAP **09**, 002 (2003).
 - [8] M. Makler, S.Q. Oliveira & I. Waga, Phys. Rev. D **64**, 123521 (2003); A. Dev, D. Jain & J.S. Alcaniz, Astron. Astrophys. **417**, 847 (2004); R. Colistete Jr. & J.C. Fabris, Class. Quant. Grav. **22**, 2813 (2005); M.C. Bento, O. Bertolami, N.M.C. Santos, A.A. Sen, Phys. Rev. D **71**, 063501 (2005).
 - [9] D. Carturan & F. Finelli, Phys. Rev. D **68**, 103501 (2003).
 - [10] H. Sandvik, M. Tegmark, M. Zaldarriaga & I. Waga, Phys. Rev. D **69**, 123524 (2004).
 - [11] L. Amendola, F. Finelli, C. Burigana & D. Carturan, JCAP **07**, 005 (2003).
 - [12] R. Bean & O. Dore, Phys. Rev. D **68**, 023515 (2003).
 - [13] R.R.R. Reis, I. Waga, M.O. Calvão & S.E. Jorás, Phys. Rev. D **68**, 061302(R) (2003).
 - [14] W. Hu, Astrophys. J. **506**, 485 (1998).
 - [15] R.R.R. Reis, M. Makler & I. Waga, Class. Quant. Grav. **22**, 353 (2005).
 - [16] M. Makler, R. R. R. Reis, L. Amendola & I. Waga, in preparation
 - [17] A.G. Riess *et al.*, Astrophys. J. **607**, 665 (2004).
 - [18] W. Freedman *et al.*, Astrophys. J. **553**, 47 (2001).
 - [19] D. Kirkman *et al.*, Astrophys. J. Suppl., **149**, 1 (2003).
 - [20] S.D.M. White & C. S. Frenk, Astrophys. J. **379**, 52 (1991); S.D.M. White, J.F. Navarro, A.E. Evrard & C. Frenk, Nature (London) **366**, 429 (1993).
 - [21] S. Sasaki, Publ. Astron. Soc. Jpn., **48**, L119 (1996).
 - [22] U. Pen, New Astronomy **2**, 309 (1997).
 - [23] S.W. Allen, R.W. Schmidt & A.C. Fabian, Mont. Not. R. Astron. Soc. **334**, L11 (2002).
 - [24] S.W. Allen *et al.*, Mont. Not. R. Astron. Soc. **353**, 457 (2004).
 - [25] D. Rappetti, S.W. Allen & J. Weller, Mont. Not. R. Astron. Soc. **360**, 555 (2005).
 - [26] G. Hinshaw *et al.* [WMAP collaboration], Astrophys. J. Suppl. **148**, 135 (2003).
 - [27] L. Verde *et al.* [WMAP collaboration], Astrophys. J. Suppl. **148**, 195 (2003).
 - [28] M. Tegmark, *et al.* [the SDSS collaboration], Phys. Rev. D **69**, 103501 (2004); M. Tegmark, *et al.* [the SDSS collaboration], Astrophys. J. **606**, 702 (2004).
 - [29] <http://space.mit.edu/home/tegmark/sdss.html>
 - [30] U. Seljak & M. Zaldarriaga, Ap. J. **469**, 437 (1996).
 - [31] R.R.R. Reis, M. Makler & I. Waga, Phys. Rev. D **69**, 101301(R) (2004).